# ADVANCED COMPUTER MODELING FOR INTERSTITIAL MICROWAVE HYPERTHERMIA THERAPY

## *Comparison of Two Numerical Methods in Computational Electromagnetics*

M. F. J. Cepeda, A. Vera, L. Leija
*Dpto. de Ingeniería Eléctrica, Sección Bioelectrónica, CINVESTAV-IPN, San Pedro Zacatenco, México D.F., México*

E. Ávila-Navarro
*Dpto. de Ciencia de Materiales, Óptica y Tecnología Electrónica. Universidad Miguel Hernández, Elche, Spain*

C. Reig, E. A. Navarro
*Dpto. de Ingeniería Electrónica, Universitat de València, Burjassot, Spain*

Keywords: Hyperthermia, Modelling, Applicator, Cancer.

Abstract: Microwave hyperthermia therapy is a recent development in the field of tumor ablation. Eelectromagnetic microwave irradiation applied to the tumor tissue causes water molecules to vibrate and rotate, resulting in tissue heating and subsequently cell death via thermal-induced protein denaturation. To effectively treat deep-stead tumors, the interstitial antennas should produce a highly localized specific absorption rate pattern and be efficient radiators at different generator frequencies. Numerical electromagnetic and thermal simulations are used to optimize the antenna design and predict heating patterns. An advanced computer modeling of a double slot antenna for interstitial hyperthermia was designed using two different numerical methods, the Finite Element Method and a Finite-difference time-domain. The aim of this work is to compare and analyze both numerical methods.

# 1 INTRODUCTION

## 1.1 Hyperthermia

Hyperthermia is a type of cancer treatment in which body tissue is exposed to high temperatures. In oncology therapeutic treatments, the cancerous cells can be destroyed if a controlled heating is induced with temperatures from 6ºC to 8ºC, with minimal injury to normal tissues. Some clinical trials have studied hyperthermia in combination with radiation therapy and/or chemo-therapy. These studies have focused on the treatment of many types of cancer as sarcoma, melanoma, and cancers of the head and neck, brain, lung, oesophagus, breast, bladder, rectum, liver, appendix, cervix, and peritoneal lining. These studies have shown a significant reduction in tumour size when hyperthermia is combined with other treatments.

## 1.2 Methods of Hyperthermia

Several methods of hyperthermia are currently under study, including local, regional, and whole-body hyperthermia.

1) Local hyperthermia is used to heat a small area, such as a tumor. It involves creating very high temperatures that destroy the cells that are heated. Radio waves, microwaves, ultrasound waves, or other forms of energy can be used to heat the area.

2) In regional hyperthermia, various approaches may be used to heat large areas of tissue, such as a body cavity, organ, or limb.

3) Whole-body hyperthermia is used to treat metastatic cancer that has spread throughout the body. This can be accomplished by several techniques that raise the body temperature, including the use of thermal chambers or hot water blankets.


Cepeda M., Vera A., Leija L., Ávila-Navarro E., Reig C. and Navarro E. (2010).
ADVANCED COMPUTER MODELING FOR INTERSTITIAL MICROWAVE HYPERTHERMIA THERAPY - Comparison of Two Numerical Methods in Computational Electromagnetics.
In *Proceedings of the Third International Conference on Biomedical Electronics and Devices*, pages 166-169
DOI: 10.5220/0002711501660169

### 1.3 Interstitial Hyperthermia

This technique allows the tumor to be heated to higher temperatures than external techniques. Under anesthesia, probes or needles are inserted into the tumor. The heat source is then inserted into the probe. For the treatment of superficial tumors the radiation is applied through external antennas, while internal tumors are exposed to invasive applicators. The operating frequency is usually 2.450 GHz, which is one of the ISM (Industrial, Scientific, and Medical) dedicated frequencies. These techniques employ implanted minimally invasive thin antennas for the delivery of local thermal doses; they are inserted through the skin, into a biocompatible catheter, under the guidance provided with an imaging monitoring procedure (Ito, 2002).

### 1.4 Numerical Methods

Three main techniques exist within computational electromagnetics (CEM). The first of these, the finite-difference time-domain (FDTD) (Yee, 1966) uses finite difference approximations of the time and space derivatives of Maxwell's curl. This method has been widely used to numerically evaluate the electromagnetic radiation patterns of antennas in tissue (Sullivan, 1990). The method of moments (MoM), approximates numerical solutions to integral equations, formulated in the frequency domain to determine an unknown current distribution for an antenna. The finite element method (FEM), has been extensively used in simulations of cardiac and hepatic radiofrequency (RF) ablation (Haemmerich, 2003). FEM models can provide users with quick, accurate solutions to multiple systems of differential equations and as such, are well suited to heat transfer problems like ablation (Bertram, 2006).

## 2 MATERIALS AND METHODS

### 2.1 Governing Equations

The frequency-dependent reflection coefficient and specific absorption rate (SAR) pattern in tissue are important for the performance of interstitial antennas. The frequency-dependent reflection coefficient, can be expressed as:

$$\Gamma(f) = 10 \cdot \log_{10}\left(\frac{P_r(f)}{P_{in}}\right) \quad [dB] \tag{1}$$

where $P_{in}$ is the input power and $P_r$ indicates reflected power (W). The frequency where the reflection coefficient is minimum is commonly referred to as the resonant frequency and should be approximately the same as the operating frequency of the generator used. SAR represents the amount of time average power deposited per unit mass of tissue (W/Kg) at any position. It can be expressed mathematically as

$$SAR = \frac{\sigma}{2\rho}\left|\overset{\vee}{E}\right|^2 \quad [W / kg] \tag{2}$$

where σ is tissue conductivity (S/m), ρ is tissue density (kg/m$^3$) and E is the electric field vector [V/m]. The tissue temperature increase results from both power and time, caused by direct MW heating (from SAR) and tissue thermal conduction. MW heating thermal effects can be roughly described by Pennes' Bioheat equation (Pennes, 1948):

$$\nabla \cdot (-k\nabla T) = \rho_b C_b \omega_b (T_b - T) + Q_{met} + Q_{ext} \tag{3}$$

where k is the tissue thermal conductivity (W/m°K), $\rho_b$ is the blood density (Kg/m$^3$), $C_b$ is the blood specific heat (J/Kg°K), $\omega_b$ is the blood perfusion rate (1/s). $T_b$ is the temperature of the blood and T is the final temperature. $Q_{met}$ is the heat source from metabolism and $Q_{ext}$ an external heat source.

### 2.2 Material Properties

The antenna is based on a 50Ω UT-085 semirigid coaxial cable. The outer conductor is copper, in which a two small ring slot of width is cut close to the short-circuited distal tip of the antenna to allow electromagnetic wave propagation into the tissue. The inner conductor is made from silver-plated copper wire (SPCW) and the coaxial dielectric used is a low-loss polytetrafluoroethylene (PTFE). Furthermore the antenna is encased in a PTFE catheter to prevent adhesion of the probe to desiccated ablated tissue. Characteristics of the materials and tissue are listed in Tab. 1.

### 2.3 Applicator Design

Antenna geometry parameters were chosen based on the effective wavelength in muscle at 2.45 GHz, which was calculated using the equation:

$$\lambda_{eff} = \frac{c}{f\sqrt{\varepsilon_r}}[m] \tag{4}$$

where c is the speed of light in free space (m/s), f is the operating frequency (2.45 GHz), and $\varepsilon_r$ = 52.729

is the relative permittivity of the tissue at the operating frequency. Fig. 1 shows that the slot spacing length corresponds to 0.25 $\lambda_{eff}$, and 0.0125 $\lambda_{eff}$ respectively, that was chose to achieve localized power deposition near the slots of the antenna.

Table 1: Dimensions and material properties for the materials and tissue.

| **Parameter** | **Value** |
|---|---|
| Center conductor diameter | 0.51 mm |
| Dielectric diameter | 1.68 mm |
| Outer conductor diameter | 2.2 mm |
| Diameter of catheter | 1.79 mm |
| Tissue electrical conductivity | 1.7388 S/m |
| Tissue thermal conductivity | 0.5 W/m°K |
| **Material** | $\varepsilon_r$ |
| Inner dielectric of the coaxial cable | 2.03 |
| Catheter | 2.60 |
| Tissue | 52.729 |

## 2.4 Computer Model Definition

### 2.4.1 Finite Element Method

Effects are modeled using commercial software package (COMSOL Multiphysics ™). The FEM model assumes that the coaxial slot antenna is immersed in homogeneous tissue. Fig. 1 shows the axial schematics of each section of the antenna, and the interior diameters. The inner and outer conductors of the antenna were modeled using perfect electric conductor boundary conditions and boundaries along the z axis are set with axial symmetry.

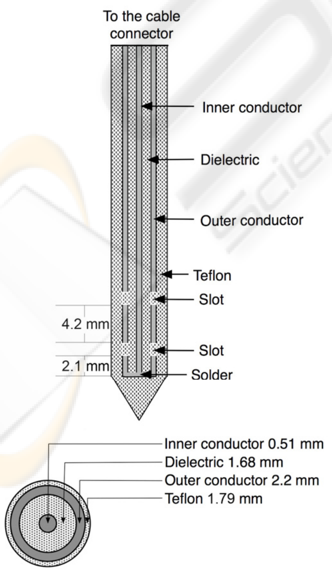


Figure 1: Shows the axial schematics of each section of the antenna, and the interior diameters.

### 2.4.2 Finite-Difference Time-Domain

The code was originally designed for the simulation of especially printed antennas (Ávila-Navarro, 2006) and recently adapted for material with losses. This is an algorithm in 3D Cartesian coordinates and full-wave in order to obtain electromagnetic fields in the time domain at any point in the simulated structure. The mesh used for the spatial discretization of the problem is configurable. By applying the Fast Fourier Transform (FFT) the field distributions is calculated in any plane, and therefore the SAR is obtained.

# 3 RESULTS

## 3.1 Finite Element Method

The mesh size was generated using the mesh parameters in Table 2. The mesh consists of 3655 triangular elements. Dense mesh zone has been generated in the vicinity of the tip of the antenna, where the temperature is more concentrated.

Table 2: Mesh parameters.

| | |
|---|---|
| Maximum element size scaling factor | 0.55 |
| Element growth rate | 1.25 |
| Mesh curvature factor | 0.25 |
| Mesh curvature cutoff | 0.0005 |

Fig. 2 shows the heat source density. The axisymmetric model requires 220 MB memory and 11 s of CPU time for single simulation on a Intel 2.4 GHz Core 2 Duo processor and a MAC OS X v10.5.7 operative system.

## 3.2 Finite-Difference Time-Domain

The simulated reflection coefficient expressed logarithmically of the coaxial double slot antenna at 2.45 GHz was -20.04. The total number of cells is approximately 587,000. The applicator is immersed in a homogeneous region simulating the human tissue. Fig. 3 shows the SAR obtained with the FDTD code for the coaxial double slot applicator used. The reflection coefficient calculated for the frequency of 2.45GHz is -11.2dB.

## 3.3 Model Validation

To validate the performance of computer model, a double slot antenna was constructed from UT-85 semirigid coaxial cable and a SMB connector. Fig. 4 shows the temperature distribution in a Cholesteric

Liquid Crystals (LCR, model NPR30C5B) at 1 W. The temperature measurement experiment setup is described in (Cepeda – 2008).

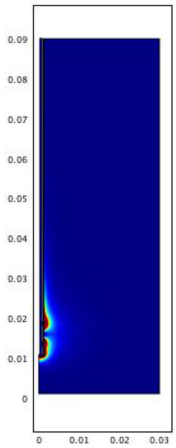


Figure 2: The computed microwave heat source density.

# 4 CONCLUSIONS

We have developed two models in parallel of an applicator for microwave hyperthermia therapy. The first of these was using commercial software based on FEM. For the other a specific code based on FDTD has been developed. Nevertheless both results are comparable. The potency of the first and versatility of the second method allows complementing and improving the design for a future application. Finally, there is an increasing need to design and evaluate applicators, which permit to improve antennas for interstitial hyperthermia using the Penne's bioheat equation.

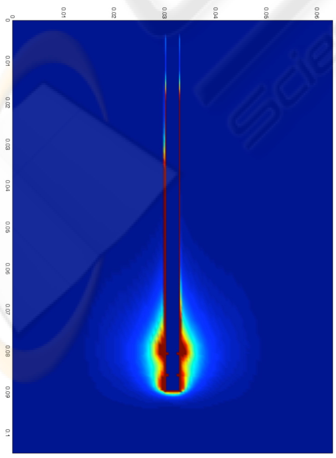

Figure 3: SAR distribution produced by FDTD.

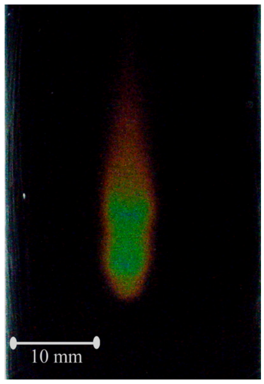


Figure 4: A picture of the hyperthermia experiment. Shows the color changes with the rise in temperature.

# REFERENCES

K. Ito, K. Saito, T. Taniguchi, H. Yoshimura, 2002. Temperature distribution in and around array applicator for interstitial microwave hyperthermia combined with interstitial radiation therapy," Proc. 27th Intl. URSI Gen. Assembly, Maastricht.

Yee KS., 1966. Numerical solution of initial boundary value problems involving Maxwell's equations in isotropic media. IEEE Trans Ant Prop, AP-14:302-307.

Sullivan D., 1990. Three-dimensional computer simulation in deep regional hyperthermia using the finite-difference timedomain method. IEEE Trans Microw Theory Tech., 38:204-211.

Haemmerich D, Chachati L, Wright AS, Mahvi DM, Lee FT, Webster JG., 2003. Hepatic radiofrequency ablation with internally cooled probes: Effect of coolant temperature on lesion size. IEEE Trans Biomed Eng., 50:493-500.

John M Bertram, Deshan Yang, Mark C Converse, John G Webster and David M Mahvi, 2006. Antenna design for microwave hepatic ablation using an axisymmetric electromagnetic model BioMedical Engineering OnLine. Biomed Eng Online 5: 15.

Wissler EH. Pennes'. 1948. Paper revisited. J Appl Physiol 1998;85(1):35–41.

E. Ávila-Navarro, J.M. Blanes, J.A. Carrasco, C. Reig, E.A. Navarro, 2006. A new bi-faced log-periodic printed antenna, Microwave and Optical Technology Letters, vol. 48, No. 2, pp. 402-405.

Cepeda M: F: J, Vera A and Leija L., Microcoaxial Double Slot Antenna for Insterstitial Hyperthermia: Modeling and Validation", International Conference on Advances in Electronics and Micro-Electronics ENICS 2008, Valencia, Spain, September, 2008, 138-143pp. ISBN: 978-0-7695-3370-4